

Electron collisions with ethylene oxide molecules

This article has been downloaded from IOPscience. Please scroll down to see the full text article.

2008 J. Phys. B: At. Mol. Opt. Phys. 41 065204

(<http://iopscience.iop.org/0953-4075/41/6/065204>)

[The Table of Contents](#) and [more related content](#) is available

Download details:

IP Address: 153.19.42.120

The article was downloaded on 25/12/2008 at 22:07

Please note that [terms and conditions apply](#).

Electron collisions with ethylene oxide molecules

Czesław Szmytkowski, Alicja Domaracka, Paweł Mozejko and Elżbieta Ptańska-Denga

Atomic Physics Group, Department of Atomic Physics and Luminescence, Faculty of Applied Physics and Mathematics, Gdańsk University of Technology, 80-952 Gdańsk, Poland

E-mail: czsz@mif.pg.gda.pl

Received 15 January 2008, in final form 13 February 2008

Published 10 March 2008

Online at stacks.iop.org/JPhysB/41/065204

Abstract

The absolute total cross section (TCS) for electron–ethylene oxide ($c\text{-C}_2\text{H}_4\text{O}$) collisions was measured at electron-impact energies extending from 0.7 to 400 eV using the linear electron-transmission technique. In the present TCS energy function a distinct peak is visible near 4.6 eV which may be attributed to formation of a short-lived negative ion. Moreover, at intermediate and high energies the integral elastic (ECS) and ionization (ICS) cross sections were determined numerically. The calculated sum, ECS + ICS, is in good agreement with the experimental TCS in the overlapping energy range. Finally, the present experimental TCS for electron scattering from $c\text{-C}_2\text{H}_4\text{O}$ is compared with that for its cyclic isoelectronic counterpart $c\text{-C}_3\text{H}_6$, and similarities and differences are pointed out and discussed.

(Some figures in this article are in colour only in the electronic version)

1. Introduction

Reliable, qualitative data on basic electron–atom/molecule collision processes are of interest in many areas of science and new technologies. Comprehensive sets of absolute electron-scattering cross sections, electron transport and rate coefficients allow for modelling reactions involved in plasma-assisted technologies, in fusion facilities, the deposition of energy by radiation in living cells, and/or processes in interstellar and environmental media (see Christophorou and Olthoff 2004, Sanche 2005, Greenberg 2002, Field 2005, and references therein).

The purpose of the present work is to provide absolute values of total, elastic and ionization cross sections describing electron–ethylene oxide molecule scattering over a wide impact energy range. Ethylene oxide is a cyclic organic compound widely used in the chemical plant industry, and as an effective fumigant and sterilant of medical devices, foodstuffs, clothing and other products. Due to the evidenced ethylene oxide mutagenicity, carcinogenicity and its high reactivity (see Report 2005), it is necessary to prevent the release of this compound into the environment. Investigations of electron-assisted processes may help in the design and construction of efficient plasma reactors to decompose the waste ethylene oxide to less harmful products (Matsumoto and Kanitani

2003, Liao *et al* 2005). Some interest in ethylene oxide comes also from recent interstellar observations (e.g. Dickens *et al* 1997).

Studies on electron-assisted processes involving ethylene oxide molecules in gas phase are still scarce and fragmentary. In the literature, one can find early experiments concerned the electron diffraction study of the $c\text{-C}_2\text{H}_4\text{O}$ molecular structure (Ackermann and Mayer 1936), the mass spectrometric analysis of positive ions (Gallegos and Kiser 1961, Holmes *et al* 1976), the electron-impact spectroscopy at intermediate energies and low scattering angles (Tam and Brion 1974), and, more recently, the study of $c\text{-C}_2\text{H}_4\text{O}$ valence electronic states with the electron momentum spectroscopy (Brunger *et al* 1995, Winkler *et al* 1999) and the electron-induced vibrational excitation and formation of resonances at low impact energies (Allan and Andric 1996). However, the obtained intensities of the observed phenomena, except those of Brunger *et al* (1995), were given only in relative units, which alone makes difficult their application for modelling of electron-assisted processes or comparison with theoretical computations. Theoretical works concerning the electron stimulated processes with $c\text{-C}_2\text{H}_4\text{O}$ molecule are not available in the literature as yet.

The present contribution reports on measurements of the accurate absolute total cross section (TCS) for energies from

0.7 to 400 eV carried out using transmission technique and on computations of integral elastic (ECS) and ionization (ICS) cross sections at intermediate and high energies, up to 3 keV, performed with the use of the additivity rule and binary-encounter-Bethe approximations, respectively. Finally, with the aim of examining how the replacement of a particular molecular atom with another one affects the TCS energy behaviour (*substitution effect*), the TCS measured for $c\text{-C}_2\text{H}_4\text{O}$ molecule has been compared with the TCS for its isoelectronic three-membered ring counterpart, $c\text{-C}_3\text{H}_6$ molecule, measured in the same laboratory (Szymkowski and Kwitniewski 2002).

2. Methods and procedures

2.1. Experimental details

In the present work, the absolute total electron-scattering cross section (TCS) was measured using the electron transmission (ET) method in a linear configuration under single collision conditions. The advantage of the transmission method is that the absolute TCS value is obtained without any normalization procedure. In the ET method the TCS is related to the attenuation of an electron beam—when passing across the target—according to the Bouguer-de Beer-Lambert (BBL) relationship

$$\text{TCS}(E) = \frac{1}{nL} \ln \frac{I(E, 0)}{I(E, n)},$$

where $I(E, 0)$ and $I(E, n)$ represent the intensities of electron beam currents, transmitted through the scattering cell, taken in the absence and presence of the target; the density number $n = p/k\sqrt{T_m T_t}$ is derived from ideal gas law using the absolute measurements of the gas target pressure (p), the temperatures of the MKS capacitance manometer head ($T_m = 322$ K) and the target cell ($T_t < T_m$) while the thermal transpiration effect has been taken into account (Knudsen 1910); L is the length of the electron pathway within the target—equal to the distance ($=30.5$ mm) between entrance and exit cell apertures, and k is the Boltzmann constant. For more details concerning the beam attenuation technique the reader is referred to the review of Bederson and Kieffer (1971).

The experimental arrangement and procedure employed in the present measurements are similar to those used extensively by us previously (e.g. Szymkowski *et al* 1997, Domaracka *et al* 2006), therefore only a short outline will be presented here. The electron beam of required energy E , with an energy spread of less than 0.1 eV (FWHM), is directed into a scattering cell filled with the target under examination. The electrons getting away from the reaction volume through the exit aperture are energy discriminated by a retarding-field analyser and eventually are collected by a Faraday cup. The molecular gas target is dosed alternately into the scattering cell or into a vacuum chamber to keep the pressure in the region of electron optics invariable throughout the experiment, irrespective of whether the target is present or absent in the cell. The electron energy scale is calibrated on the well-known resonant oscillatory structure in N_2 observed around 2.3 eV (e.g. Szymkowski *et al* 1996). To ensure that the electron

trajectory in the spectrometer is not disturbed by a magnetic field, its intensity is reduced to a value below 100 nT.

The final TCS value at each given electron-impact energy is a weighted mean of results from several series, each containing up to ten individual runs, performed at a variety of target pressures, p , from about 20 to 160 mPa. The statistical uncertainty (one standard deviation of the weighted mean value) of the resulting absolute TCS does not exceed 1% over the whole energy range used. More serious are uncertainties of systematic character. In the ET method, the electron current intensity $I(E, n)$ is systematically overestimated due to inability to discriminate against electrons which are scattered elastically through small angles in the forward direction; these electrons contribute to the transmitted signal and may lower the measured TCS by 2–4% in the present experiment. Moreover, the effusion of the target molecules through orifices of the reaction cell gives rise to an error of about 1% (see Nelson and Colgate 1973) in establishing the real value of the factor nL in the BBL formula. Below 2 eV, where the TCS is a steep function of energy, an extra error of 3–5% may arise due to an uncertainty of about 0.1 eV in the energy scale. The comprehensive analysis of particular components of the systematic uncertainty has been already discussed elsewhere (Szymkowski *et al* 1997). The overall systematic uncertainty in the determined TCS, estimated as a combination of potential systematic errors of measured individual quantities, is about 7–9% below 2 eV, decreasing gradually to 3–4% between 6 and 100 eV, and increasing to 5–6% at higher energies. A commercially supplied sample of ethylene oxide (Fluka), with a purity of 99.8%, was used directly from the container without further purification.

2.2. Computational

Complementary to the experimental investigations, we have performed simple but quite reliable numerical calculations of the ionization and integral elastic cross sections for electron scattering from the $c\text{-C}_2\text{H}_4\text{O}$ molecule. Theoretical methods employed in the present work have been presented in our earlier studies (Mozejko *et al* 2002, Mozejko and Sanche 2003); therefore, we will provide only a brief description here.

The ionization cross section has been calculated using the binary-encounter-Bethe (BEB) model (Hwang *et al* 1996). Within that approach the electron-induced total ionization cross section for a molecule, σ^{Ion} , can be obtained as the sum of cross sections for ionization of each individual molecular orbital, σ_i^{BEB} , i.e.

$$\sigma^{\text{Ion}} = \sum_{i=1}^{n_{\text{MO}}} \sigma_i^{\text{BEB}},$$

where n_{MO} is the number of molecular orbitals. The electron-impact ionization cross section per molecular orbital can be derived according to the following equation:

$$\sigma^{\text{BEB}} = \frac{S}{\epsilon + u + 1} \left[\frac{\ln \epsilon}{2} \left(1 - \frac{1}{\epsilon^2} \right) + 1 - \frac{1}{\epsilon} - \frac{\ln \epsilon}{\epsilon + 1} \right],$$

where $u = U/B$, $\epsilon = E/B$, $S = 4\pi a_0^2 N R^2 / B^2$, $a_0 = 0.5292$ Å, $R = 13.61$ eV and E is the energy of the

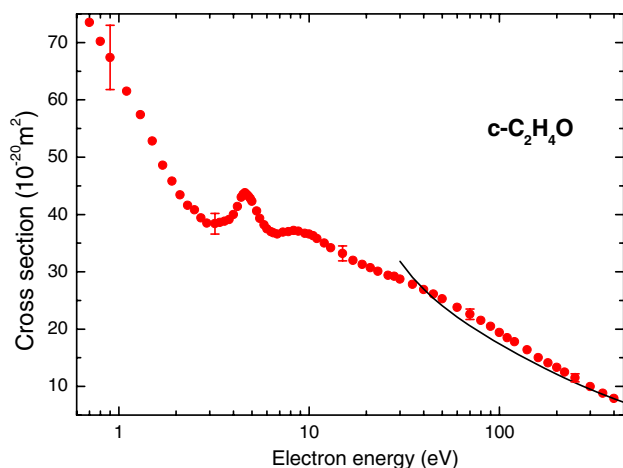


Figure 1. Total cross sections for electron scattering from the $c\text{-C}_2\text{H}_4\text{O}$ molecule: (●), present experimental TCS (error bars represent overall, systematic plus statistical, uncertainties); (—), sum of calculated elastic (ECS) and ionization (ICS) cross sections, present.

incident electron. All molecular parameters, i.e. the electron binding energy, B , kinetic energy of the orbital, U , and orbital occupation number, N , have been calculated for the ground state of the geometrically optimized, within C_{2v} symmetry, $c\text{-C}_2\text{H}_4\text{O}$ molecule at the Hartree–Fock level using the GAUSSIAN code (Frisch *et al* 2003) and Gaussian 6-311G + basis set. Moreover, the ionization energies of the valence orbitals have been computed using outer valence Green function calculations (Zakrzewski and von Niessen 1994).

The elastic electron interaction with the $c\text{-C}_2\text{H}_4\text{O}$ molecule has been studied with the additivity rule (e.g. Raj 1991, Joshipura and Patel 1994) in which the molecular elastic cross section is calculated from individual cross sections for elastic electron scattering on atomic components of the molecule.

To obtain cross sections for elastic electron scattering from particular atoms the radial Schrödinger equation

$$\left[\frac{d^2}{dr^2} - \frac{l(l+1)}{r^2} - 2(V_{\text{stat}}(r) + V_{\text{polar}}(r)) + k^2 \right] u_l(r) = 0$$

has been solved numerically and standard partial wave analysis has been performed. In calculations, the electron–atom interaction has been represented by static $V_{\text{stat}}(r)$ (Salvat *et al* 1987) and the polarization $V_{\text{polar}}(r)$ (Padias and Norcross 1984, Perdew and Zunger 1981) potentials, and the exact phase shifts have been calculated for l up to $l_{\text{max}} = 50$, while those remaining have been included through the Born approximation; polarizability values have been taken from Lide (1995–1996).

Final values of computed integral elastic (ECS) and ionization (ICS) cross sections for electron scattering from ethylene oxide molecule are presented in table 2 and their sum, ECS+ICS, is compared in figure 1 with the total cross section (TCS) measured in this work.

Table 1. Absolute experimental electron-scattering total cross sections for $c\text{-C}_2\text{H}_4\text{O}$ molecules; in units of 10^{-20} m^2 .

E (eV)	TCS	E (eV)	TCS	E (eV)	TCS	E (eV)	TCS
0.7	73.5	4.2	41.4	8.8	37.1	50	25.3
0.8	70.2	4.4	43.0	9.5	36.7	60	23.8
0.9	67.4	4.5	43.5	10.0	36.6	70	22.6
1.1	61.5	4.6	43.8	10.5	36.3	80	21.5
1.3	57.4	4.7	43.5	11	35.8	90	20.5
1.5	52.8	4.8	43.2	12	35.0	100	19.4
1.7	48.6	4.9	42.8	13	34.2	110	18.5
1.9	45.8	5.0	42.3	15	33.2	120	17.8
2.1	43.4	5.3	40.6	17	32.0	140	16.4
2.3	41.6	5.5	39.3	19	31.3	160	15.0
2.5	40.8	5.8	38.2	21	30.7	180	14.1
2.7	39.4	6.0	37.5	23	30.1	200	13.3
2.9	38.5	6.3	37.0	26	29.4	220	12.5
3.2	38.4	6.5	36.8	28	29.2	250	11.5
3.4	38.6	6.8	36.6	30	28.7	300	9.96
3.6	38.8	7.3	36.9	35	27.8	350	8.79
3.8	39.1	7.8	37.0	40	26.9	400	7.91
4.0	40.0	8.3	37.2	45	26.1		

3. Results and discussion

3.1. Ethylene oxide, $c\text{-C}_2\text{H}_4\text{O}$

Figure 1 shows our absolute total cross section (TCS) for electron scattering by ethylene oxide molecule, measured for incident energies between 0.7 and 400 eV. At intermediate energies the experimental TCS data are compared with calculated, in this work, the cross section composed as a sum of computed integral elastic (ECS) and ionization (ICS) cross sections. Table 1 supplies the numerical TCS values obtained in the present experiment, while table 2 gives the ECS and ICS calculated at intermediate and high energies.

Considering the energy dependence of the experimental TCS curve presented in figure 1, four regions are distinguishable over the energy range examined.

- (i) At the lowest applied energies the measured TCS decreases rapidly with the energy increase, from nearly $74 \times 10^{-20} \text{ m}^2$ at 0.7 eV down to the local minimum value of about $38 \times 10^{-20} \text{ m}^2$ at 3.2 eV. Such low-energy behaviour of the electron-scattering TCS is rather common for molecules of high permanent electric dipole moment (for $c\text{-C}_2\text{H}_4\text{O}$ $\mu = 1.89 \text{ D}$, Lide 1995–1996) and is explained in terms of the charge-dipolar moment potential scattering.
- (ii) Between two minima located at 3.2 and 6.8 eV, the TCS curve reveals a distinct resonant-like peak with the maximum value of $44 \times 10^{-20} \text{ m}^2$ near 4.6 eV. This feature can be attributed to the formation of short-lived negative-ion state (*resonance*) when the approaching electron is captured temporarily by the $c\text{-C}_2\text{H}_4\text{O}$ molecule into an unoccupied energy level. The resonance then decays through the auto-detachment of the extra electron leaving the parent molecule in the vibrational level of the ground electronic state or may decompose into negative and neutral fragments. The lifetime of the 4.6 eV resonance with respect to the electron auto-detachment, estimated from the width of the resonant peak, is about 1 fs and

Table 2. Ionization (ICS) and integral elastic (ECS) cross sections calculated for electron impact on *c*-C₂H₄O molecules; in units of 10⁻²⁰ m².

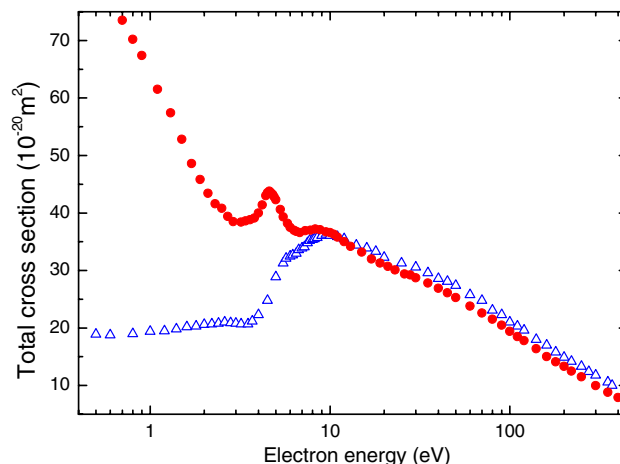
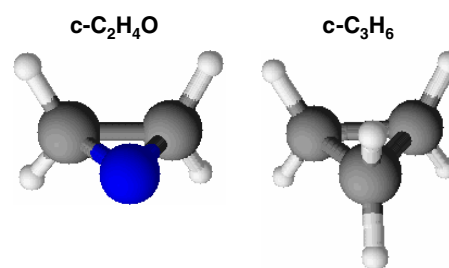
E (eV)	ICS	E (eV)	ICS	ECS	E (eV)	ICS	ECS
10.502	0.00	30	4.29	27.5	200	5.55	6.59
11	0.0373	35	5.01	24.0	250	5.01	5.63
12	0.153	40	5.55	21.4	300	4.55	4.94
13	0.311	45	5.96	19.4	350	4.17	4.42
14	0.488	50	6.26	17.8	400	3.85	4.00
15	0.748	60	6.63	15.5	450	3.58	3.66
16	1.00	70	6.81	13.8	500	3.34	3.38
17	1.27	80	6.86	12.5	600	2.96	2.93
18	1.56	90	6.84	11.5	700	2.65	2.59
19	1.85	100	6.78	10.6	800	2.41	2.33
20	2.13	110	6.68	9.96	900	2.21	2.11
22.5	2.76	120	6.57	9.38	1000	2.04	1.94
25	3.32	140	6.32	8.43	1500	1.50	1.39
27.5	3.84	160	6.06	7.69	2000	1.19	1.11
		180	5.80	7.09	2500	0.991	0.971
					3000	0.853	0.913

exceeds the time the impinging electron needs to pass the distance equal to molecular diameter. The 4.6 eV TCS structure can be related to the distinct narrow peak observed earlier by Allan and Andric (1996) around 4.8 eV in the electron-excitation functions of the ring stretch vibrations of the *c*-C₂H₄O molecule, and attributed to the formation of the shape resonance.

- (iii) Above 7 eV the TCS curve has a weak enhancement, extending to more than 12 eV, peaking close to 8.5 eV with a value of $37 \times 10^{-20} \text{ m}^2$. According to the experiment of Allan and Andric (1996), this enhancement may be also related to the resonant scattering leading to the excitation of the CH stretching and the CH₂ scissoring vibrations of parent molecule in its electronic ground state.
- (iv) Behind 9 eV the TCS decreases continuously with energy down to $8 \times 10^{-20} \text{ m}^2$ at 400 eV. Worth noting is the change of the slope of the TCS curve visible within 20–40 eV. The origin of this feature may be related in part to the presence of numerous weak resonances in this energy region but it may also arise due to direct processes allowed at these energies, especially the ionization. Starting from 70 eV, the energy dependence of the experimental TCS for electron–ethylene oxide scattering behaves like $\sim E^{-0.6}$.

Finally, a barely discernible but repetitive shoulder around 2.7 eV, on the descending slope of TCS curve, is also worth mentioning as it may correspond to the weak resonant structure perceived in DCS near 3 eV by Allan and Andric (1996).

As shown in figure 1, a sum of calculated ECS and ICS is in good agreement with the experimental TCS. Generally, the computed representation of total cross section is lower than the measurements. However, differences between experiment and calculations do not exceed 10% and above 200 eV both curves come to merge to within 1% when the energy approaches 400 eV. Such agreement allows us to expect that the computed cross sections may give a credible estimation of the scattering quantities also at energies behind the upper limit of the present experiment.

**Figure 2.** Comparison of experimental total cross sections for electron scattering from: *c*-C₂H₄O (●), present; *c*-C₃H₆ (Δ), Szmytkowski and Kwitniewski (2002).**Figure 3.** Schematic representation of *c*-C₂H₄O and *c*-C₃H₆ molecules in their ground state.

3.2. Comparison of electron-scattering TCSs for *c*-C₂H₄O and *c*-C₃H₆ molecules

In figure 2, we compare the TCS for electron scattering from *c*-C₂H₄O molecule with that for *c*-C₃H₆ (Szmytkowski and Kwitniewski 2002). As these compounds have different ring components—the oxygen atom in *c*-C₂H₄O is replaced with CH₂ group in *c*-C₃H₆ (see figure 3)—differences in the energy dependence of their TCSs are expected, more and more prominent towards lower impact energies.

Indeed, while below 3 eV the TCS for *c*-C₃H₆ is almost constant, approx. $20 \times 10^{-20} \text{ m}^2$ (in fact, it even slowly decreases towards 0.6 eV), the TCS for *c*-C₂H₄O increases steeply towards lower energies almost twofold, from about $38 \times 10^{-20} \text{ m}^2$ in the vicinity of 3.2 eV to nearly $74 \times 10^{-20} \text{ m}^2$ at 0.7 eV. This dissimilarity can be related to substantial difference between long-range contributions to the electron–molecule interaction for both molecular targets. The replacement of one CH₂ group in the *c*-C₃H₆ molecule with an oxygen atom significantly disturbs the symmetry of charge distribution in the resultant molecule. In consequence, the *c*-C₂H₄O molecule has quite a large permanent electric dipole moment, 1.89 D, while *c*-C₃H₆ is nonpolar in its ground state. That is clearly reflected in the experimental TCS low-energy function.

Table 3. A comparison of selected parameters for c-C₂H₄O and c-C₃H₆ molecules (Lide 1995-1996): permanent electric dipole moment (μ), electrical polarizability (α), the gas-kinetic cross section (σ_{gk}) estimated using the van der Waals constant, bond lengths and angles.

Molecule	μ (Debye)	α (10^{-30} m ³)	σ_{gk} (10^{-20} m ²)	Bond length (Å)	Angle (°)
c-C ₂ H ₄ O	1.89	4.43	11.2	C—C 1.466	HCH 116.6
				C—H 1.085	
				C—O 1.431	
c-C ₃ H ₆	0	5.66	11.9	C—C 1.512	HCH 114.0
				C—H 1.083	

Another interesting difference between compared TCSs concerns the appearance of the resonant features. In the TCS curve for c-C₃H₆ there is a weak shoulder barely discernible near 6 eV (see also Winstead *et al* 1992, Beyer *et al* 1997, Ćurik and Gianturco 2002, Makochekanwa *et al* 2006) while for c-C₂H₄O, a distinct peak appears around 4.6 eV. These TCS structures correspond, respectively, to pronounced peaks observed by Allan and Andric (1996) in the vibrational inelastic differential cross sections (DCSs) at 5.5 eV for c-C₃H₆ and at 4.8 eV for c-C₂H₄O. Both c-C₃H₆ and c-C₂H₄O DCS peaks were attributed to the formation of shape resonant states which lead to the excitation of the ring stretch vibrations with possible activation of the C–H stretching and CH₂ scissoring modes of the related parent molecules. However, in contrast to the resonant features in the compared TCSs, the respective structures in DCSs look much the same—they are very distinct and similar.

On the other hand, both c-C₂H₄O and c-C₃H₆ molecules are isoelectronic, they are three-membered rings (C–O–C and C–C–C, with each carbon being fully hydrogenated, cf figure 3) and have nearly equal gas-kinetic cross section (see table 3). Therefore, one would expect also some similarities in their TCS behaviour, mainly at higher impact energies. With the increasing energy, the impinging electron experiences the target molecule as a cluster of individual atoms rather than as a whole. Then the charge distribution and/or arrangement of atoms in the molecule become less important and the independent atom approximation becomes valid (cf Mott and Massey 1965). As seen in figure 2, starting from the 8–10 eV maxima, TCSs for both compounds have very similar shape and differ in the magnitude only slightly; above 15 eV the TCS for c-C₃H₆ is systematically higher by about 1.5×10^{-20} m² as the consequence of somewhat larger size of the c-C₃H₆ molecule.

4. Concluding remarks

In ethylene oxide we have measured the absolute electron-scattering total cross section (TCS) within the 0.7–400 eV incident energy range. The obtained TCS shows a distinct maximum centred near 4.6 eV which can be explained as the resonant effect. We have also calculated elastic (ECS) and ionization (ICS) cross sections at intermediate and high impact energies up to 3 keV. Sum of ECS and ICS is in good agreement with the experimental TCS at overlapping energies. Some similarities and differences between TCSs for c-C₂H₄O molecule and its cyclic and isoelectronic counterpart c-C₃H₆ have been pointed out and discussed.

Acknowledgments

This work is part of the MNSzW programme 2007–2008 and is supported by the Polish Ministry of Science and Higher Education (project no N202 110 32/2862). Numerical calculations have been performed at the Academic Computer Centre (TASK) in Gdańsk.

References

- Ackermann G and Mayer J E 1936 *J. Chem. Phys.* **4** 377–81
Allan M and Andric L 1996 *J. Chem. Phys.* **105** 3559–68
Bederson B and Kieffer L J 1971 *Rev. Mod. Phys.* **43** 601–40
Beyer T, Nestmann B M, Sarpal B K and Peyerimhoff S D 1997 *J. Phys. B: At. Mol. Opt. Phys.* **30** 3431–44
Brunger M J, Weigold E and von Niessen W 1995 *Chem. Phys. Lett.* **233** 214–19
Christophorou L G and Olthoff J K 2004 *Fundamental Electron Interactions with Plasma Processing Gases* (New York: Kluwer)
Ćurik R and Gianturco F A 2002 *J. Phys. B: At. Mol. Opt. Phys.* **35** 717–32, 1235–50
Dickens J E, Irvine W M, Ohishi M, Ikeda M, Ishikawa S, Nummelin A and Hjalmarsen Å 1997 *Astrophys. J.* **489** 753–7
Domaracka A, Możejko P, Ptasińska-Denga E and Szmytkowski Cz 2006 *J. Phys. B: At. Mol. Opt. Phys.* **39** 4289–99
Gallegos E J and Kiser R W 1961 *J. Am. Chem. Soc.* **83** 773–7
Greenberg J M 2002 *Surf. Sci.* **500** 793–822
Field D 2005 *Europhys. News* **36** 51–5
Frisch M J *et al* 2003 *GAUSSIAN 03*, revision B.03 (Pittsburgh, PA: Gaussian, Inc.)
Holmes J L, Terlouw J K and Lossing F P 1976 *J. Phys. Chem.* **80** 2860–2
Hwang W, Kim Y K and Rudd M E 1996 *J. Chem. Phys.* **104** 2956–66
Joshiyura K N and Patel P M 1994 *Z. Phys. D* **29** 269–73
Knudsen M 1910 *Ann. Phys., Lpz.* **31** 205–29
Liao W T, Wei T C, Hsieh L T, Tsai C H and Shih M 2005 *Aerosol Air Qual. Res.* **5** 185–203
Lide D R (ed) 1995-1996 *CRC Handbook of Chemistry and Physics* 76th edn (Boca Raton, FL: CRC Press)
Makochekanwa C, Kato H, Hoshino M, Tanaka H, Kubo H, Bettiga M H F, Lopes A R, Lima M A P and Ferreira L G 2006 *J. Chem. Phys.* **124** 024323
Matsumoto K and Kanitani M 2003 *IEEE Conf. Record-Abstracts: 30th Int. Conf. on Plasma Science (Jeju, Korea)* p 285
Mott N F and Massey H S W 1965 *The Theory of Atomic Collisions* (Oxford: Oxford University Press)
Możejko P, Żywicka-Możejko B and Szmytkowski Cz 2002 *Nucl. Instrum. Methods Phys. Res. B* **196** 245–52
Możejko P and Sanche L 2003 *Radiat. Environ. Biophys.* **42** 201–11
Nelson R N and Colgate S O 1973 *Phys. Rev. A* **8** 3045–9
Padial N T and Norcross D W 1984 *Phys. Rev. A* **29** 1742–8
Perdew J P and Zunger A 1981 *Phys. Rev. B* **23** 5048–79
Raj D 1991 *Phys. Lett. A* **160** 571–4

- Report on Carcinogens* 2005 11th edn, US Department of Health and Human Services, Public Health Service, National Toxicology Program
- Salvat F, Martinez J D, Mayol R and Parellada J 1987 *Phys. Rev. A* **36** 467–74
- Sanche L 2005 *Eur. J. Phys. D* **35** 367–90
- Szmytkowski Cz, Macig K and Karwasz G P 1996 *Phys. Scr.* **54** 271–80
- Szmytkowski Cz, Mozejko P and Kasperski G 1997 *J. Phys. B: At. Mol. Opt. Phys.* **30** 4363–72
- Szmytkowski Cz and Kwitniewski S 2002 *J. Phys. B: At. Mol. Opt. Phys.* **35** 2613–23
- Tam W C and Brion C E 1974 *J. Electron Spectrosc. Relat. Phenom.* **3** 263–79
- Winkler D A, Michalewicz M T, Wang F and Brunger M J 1999 *J. Phys. B: At. Mol. Opt. Phys.* **32** 3239–53
- Winstead C, Sun Q and McKoy V 1992 *J. Chem. Phys.* **96** 4246–51
- Zakrzewski V G and von Niessen W 1994 *J. Comp. Chem.* **14** 13–8